A Dimeric Peptide That Binds Selectively to Prostate-Specific Membrane Antigen and Inhibits its Enzymatic Activity

Saurabh Aggarwal,[1] Pratap Singh,[2] Ozlem Topaloglu,[1] John T. Isaacs,[1,2] and Samuel R. Denmeade[1,2]

[1]The Sidney Kimmel Comprehensive Cancer Center, The Johns Hopkins University School of Medicine and [2]Chemical and Biomolecular Engineering Department, The Johns Hopkins University Whiting School of Engineering, Baltimore, Maryland

Abstract

Prostate-specific membrane antigen (PSMA) is highly expressed by both normal and malignant prostate epithelial cells and by the neovasculature of many tumor types; however, it is not expressed by normal endothelial cells or other normal tissues. PSMA, therefore, represents an attractive candidate for selectively targeted therapies for prostate and/or other solid tumors. As an alternative approach to antibody-based anti-PSMA therapies, small peptides that bind selectively to PSMA-producing cells can be used to deliver cytotoxic drugs, protein toxins, and viruses selectively to malignant sites while minimizing systemic toxicity to normal tissues. Small peptides are relatively inexpensive to produce, not immunogenic, and easily coupled to cytotoxic agents. In the present study, a random phage library consisting of linear 12 amino acid peptides was used to identify peptides that bound selectively to PSMA. From a series of monomeric peptides, one with the sequence WQPDTAHHWATL was used to show binding of soluble peptide to PSMA. A dimeric version of this peptide showed markedly enhanced binding to soluble PSMA and an IC_{50} of 2.2 μmol/L for inhibition of PSMA enzymatic activity. Fluorescently labeled dimeric peptide bound selectively to PSMA-producing prostate cancer cells *in vitro* with no significant binding to non–PSMA-producing cells. Molecular modeling of the dimeric peptide revealed that histidine residues in close vicinity can efficiently coordinate a divalent ion and hold the peptide in a favorable configuration for binding and subsequent inhibition. These dimeric peptides, therefore, represent putative PSMA-selective targeting agents that are currently being evaluated for selective binding *in vivo*. (Cancer Res 2006; 66(18): 9171-7)

Introduction

Prostate-specific membrane antigen (PSMA) is a 100 kDa prostate epithelial cell type II transmembrane glycoprotein that is expressed by normal prostate epithelium and by a large proportion of primary and metastatic prostate cancers (1–3). PSMA has an extracellular domain that is accessible to agents in the extracellular peritumoral fluid, making it possible to target this protein with antibodies and prodrugs (4, 5). Recent crystal structural analyses showed that PSMA exists as a homodimer with structural homology to the transferrin receptor (6, 7). Low levels of PSMA expression can be detected in other tissues, including the brain, kidney, liver, and small intestine (3). In all other human tissues, including normal vascular endothelium, PSMA expression has not been detected (1, 8, 9). PSMA expression has been undetectable in other nonprostatic primary tumors (1–3). Others, however, have shown low-level PSMA expression in primary renal and transitional cell carcinomas (10, 11).

Several groups have also shown PSMA expression in the neovasculature of a variety of tumor types, including renal, bladder, colon, neuroendocrine, pancreatic, and lung cancers, and the majority of breast cancers and sarcomas (3, 12, 13). Huang et al. (14) used an antibody against mouse PSMA to further show expression in human tumor neovasculature but no expression of PSMA in mouse endothelial cells present within human or mouse-derived tumor xenografts. Finally, phase I studies in patients with a variety of cancer types using ^{111}In-labeled PSMA antibodies showed localization of labeled antibody to tumor sites in 15 of 19 patients (79%), which occurred in metastatic sites in viscera, soft tissue, and bone (15).

The aforementioned studies highlight some of the characteristics of PSMA that make it a suitable target for prostate-specific therapy as well as a potential target for all solid tumors. A radiolabeled anti-PSMA antibody is currently used clinically as a diagnostic tool for the detection of recurrent prostate cancer (i.e., Prostascint scan). As an alternative approach to antibody-based anti-PSMA therapies, we are proposing instead to use small peptides that bind selectively to PSMA-producing prostate cancer cells and endothelial cells within solid tumors. The advantages of small binding peptides are that they are relatively inexpensive to produce, not highly immunogenic, stable, and can be easily coupled to cytotoxic agents. Examples of such conjugates include luteinizing hormone-releasing hormone peptide coupled to cytotoxic agents, such as doxorubicin, or small lytic peptides (16, 17). Protein-specific-binding peptides can also be incorporated into the coat protein of viruses to generate targeted protein toxins or viral therapies (18). These binding peptides could also be used to capture circulating cancer cells from the bloodstream as an alternative to biopsies and could also be used to image PSMA cells (19).

The goal, therefore, of the present study was to identify small peptides of 12 amino acids that bound selectively to PSMA that could be used to target cytotoxic agents, to image or to capture PSMA-producing cells. In this study, phage display was used to identify a candidate peptide that bound selectively to PSMA. This peptide was found to inhibit the carboxypeptidase activity of PSMA. Dimerization of this peptide resulted in enhanced binding to PSMA and ~10-fold better inhibition of PSMA activity compared with the monomeric peptide. In addition, the selected dimeric peptide specifically bound to PSMA-producing prostate cancer cells with no significant binding to non–PSMA-producing cells.

Materials and Methods

Materials. M13 Phage Display System of 12-mer random library was from New England Biolabs (Beverly, MA). Magnetic beads with anti-His

Requests for reprints: Samuel R. Denmeade, Department of Oncology, Bunting Blaustein Cancer Research Building, 1650 Orleans Street, Baltimore, MD 21231. Phone: 410-502-3941; Fax: 410-614-8397; E-mail: denmesa@jhmi.edu.

doi:10.1158/0008-5472.CAN-06-1520

antibody (His-MACS) were from Miltenyi Biotec (Auburn, CA). *Drosophila* expression system was from Invitrogen (Rockville, MD). Anti-M13-horseradish peroxidase (HRP) conjugate was from Amersham Pharmacia Biotech (Buckinghamshire, United Kingdom). All peptide synthesis reagents were from Anaspec (San Jose, CA). Unless otherwise indicated, all the other reagents were from Sigma-Aldrich (St. Louis, MO).

Cell lines. The LNCaP, PC-3, and DU-145 human prostate cancer cell lines (American Type Culture Collection, Rockville, MD) and CWR22R cells (Dr. John Isaacs, Johns Hopkins University, Baltimore, MD) were maintained by serial passage in RPMI 1640 (Life Technologies, Grand Island, NY) containing 10% fetal bovine serum (FBS; Bio-Whittaker, Walkersville, MD) in 5% CO_2/95% air at 37°C.

PSMA cloning and expression. A PCR approach was used to amplify and attach His-6 tag to amino terminus of extracellular domain of PSMA. Primers used were (forward *Bgl*II) 5′-GGA*AGATCT*CATCATCATCACCATTCACCATAAATCCTCCAATGAAGC-3′ and (reverse *Xho*I) 5′-GGC-*CTCGAG*TCATTAGGCTACTTCACTCAAAG-3′. Template amplification was done using Pfu-polymerase (Promega, Madison, WI) as per suggested protocol. A PCR reaction began with an initial denaturation step (94°C for 2 minutes) followed by three cycles of amplification (94°C for 30 seconds, 40°C for 1 minute, 72°C for 2 minutes), followed by 30 cycles of amplification (94°C for 30 seconds, 58°C for 1 minute, 72°C for 2 minutes), and ended with a final extension step (72°C for 10 minutes). A 2,136 bp PCR fragment was purified by gel electrophoresis, digested with *Bgl*II/*Xho*I and cloned into pMT/BiP/V5-HisA (Invitrogen) previously digested with same set of enzymes. Final construct was designated as pMT-His-PSMA.

His-tagged PSMA large-scale expression and purification. Schneider's S2 cells (Invitrogen) were maintained in *Drosophila* expression system medium (Life Technologies, Rockville, MD) supplemented with 10% FBS at 28°C. The cells were cotransfected with pMT-His-PSMA and pCoHYGRO (19:1 ratio) selection vector using calcium phosphate–mediated transfection kit (Invitrogen). His-PSMA was purified from conditioned medium by incubating with Ni-NTA resin (Qiagen, Valencia, CA) in manufacturer-recommended salt and imidazole concentration. PSMA was eluted using 250 mmol/L imidazole and purity checked by SDS-PAGE Coomassie staining. Western blot was probed with anti-His Tag [Penta-His-HRP conjugate (Qiagen) and anti-PSMA (Yes Biotech, Ontario, Canada)] mouse monoclonal antibodies.

Phage library screening. Peptides from the random M13 12-mer phage library were selected using His-tagged PSMA as the target, which was then captured using magnetically labeled anti-His Tag antibody. To remove nonspecific phage binding to anti-His antibody and other components of the magnetic separation system, the library was depleted twice with the His-MACS system. First round of screening: The final eluate from negative screening was incubated with 0.8 μg PSMA for 30 minutes at room temperature. Fifty microliters of His-MACS were added and allowed to bind for 30 minutes at room temperature. The incubation mixture was loaded onto a MACS column and washed twice with 1 mL PBS/0.1% Tween 20 (PBST). Beads containing PSMA bound to phage were collected and amplified using PhD kit protocol (NEB, Auburn, MA). Second round screening: Negative screening was repeated as above except with more bovine serum albumin (BSA; 0.5%) and longer incubation (1 hour at 4°C). From the first round of screen, 10^{10} plaque-forming units (pfu) were then incubated with PSMA in 1% BSA for 6 hours at 4°C. His-MACS in 3% BSA were incubated for 30 minutes and bound phages were collected and amplified as in round one. For third round screening, the same method was used except that mouse IgG solution (100 μg/mL) was added to the blocking solution. Individual phage were selected and sequenced after third round of screening.

Peptide synthesis. Peptides were synthesized using standard solid phase Fmoc chemistry on Wang resin as previously described (20). Dimeric peptide was synthesized by coupling Fmoc-Lys-(Fmoc) to Lys-(ε-Biotin or FITC)-Wang resin. Peptides were purified using reverse phase-high pressure liquid chromatography and sequences confirmed by matrix-assisted laser desorption/ionization-time of flight mass spectroscopy.

PSMA enzymatic assay. The enzymatic activity assay for PSMA was adapted as previously described by Tiffany et al. (21). PSMA (5 nmol/L) incubated with or without peptides was added to PSMA assay buffer [10 mmol/L $CoCl_2$, 50 mmol/L Tris (pH 7.4)]. Following a 30-minute incubation at 37°C, *N*-acetyl-aspartyl-3*H* glutamate (^{3}H-NAAG; NEN, Boston, MA) was added to final concentration of 25 nmol/L and reactions were incubated for 15 minutes at 37°C. Data were collected during linear phase of hydrolysis (i.e., <20% cleavage of total substrate).

Phage ELISA. The phage displaying a specific peptide was amplified and purified and peptide display was confirmed by DNA sequencing. The titer value of the specific purified phage was determined and three different dilutions were prepared in 1% BSA in PBST. PSMA (0.625 μg) was coated on 96-well polystyrene ELISA plates blocked with 3% BSA in PBST at 37°C for 2 hours. Phage dilutions were incubated for 1 hour at room temperature. For competitive assay, PSMA phages at 10^{10} pfu/mL were first incubated at room temperature for 1 hour with 500 nmol/L PSMA. Blocking solution was then removed from wells and phage dilutions were incubated for 1 hour at room temperature. After 7× washing, anti-M13-HRP conjugate (1:500) in 3% BSA in PBST was incubated for 30minutes. After a second wash (7× PBST), the HRP substrate *O*-phenylenediamine dihydrochlroride (OPD) was added and absorbance was measured at 450 nm.

Reverse ELISA. Streptavidin-coated 96-well plates were blocked with 2% BSA in PBST for 1 hour. After washing, biotinylated peptide monomer and the dimeric peptide were incubated at a final concentration of 25 μmol/L for 2 hours. After washing, PSMA 100 nmol/L in 3% BSA was incubated for 2 hours at room temperature. Wells were washed 6× with PBST and anti-penta-His-HRP conjugate (1:1,000) in 3% BSA was incubated for 1 hour. Substrate 2,2′-azino-bis(3-ethylbenzthiazoline-6-sulfonic acid) was added and absorbance was measured at 405 nm after 30 minutes.

Structural modeling. The MOE program (CCG, Montreal, Quebec, Canada) was used to build monomeric as well as dimeric peptide. The minimization of the dimer was done in the presence of Cobalt cation using OPLS-AA force field. The continuum solvent model was used to mimic the solvent effects. GOLD v3.0 program (CCDC, Cambridge, United Kingdom) was used to dock the peptide moiety in the binding site of PSMA. The crystal structure of PSMA dimer (Protein Data Bank code 1Z8L) was used to extract the coordinates for the protein monomer for subsequent docking. GOLD program uses a genetic docking program for flexible docking of ligands into protein binding sites. This program has been shown to produce accurate results for many protein-ligand systems, including metalloproteases. The default variables in the GOLD program were used to perform all docking runs. The binding site was defined by a radius of 25 Ångstrom from the catalytic site, which is large enough for the peptide to sample all the binding sites in the vicinity of catalytic site.

Results

Identification of PSMA-binding peptides. To screen for peptides that bind only to the extracellular domain of PSMA, recombinant PSMA lacking the transmembrane and intracellular domain was generated. Purified His-PSMA ran as single band on a Coomassie-stained gels and was visualized by Western blotting using anti-PSMA mouse monoclonal antibody (data not shown). His-PSMA released [^{3}H]Glu from the [^{3}H]NAAG substrate at a rate of 61 ± 8 nmol ^{3}H Glu/min/mg protein. This purified, enzymatically active His-PSMA was used for all subsequent binding experiments.

To decrease the selection of nonspecific low-affinity binders, phage screening was done in solution and incorporated negative screening steps using other selection components (i.e., antibodies, magnetic beads, etc.) to remove many background binders (22). Thus, for this study, the phage library was incubated with magnetically labeled anti-His_6 antibody after every round of selection. After negative selection steps, His-PSMA was incubated with the phage library and phages bound to His-PSMA were captured using magnetically labeled anti-His_6 antibody (Fig. 1).

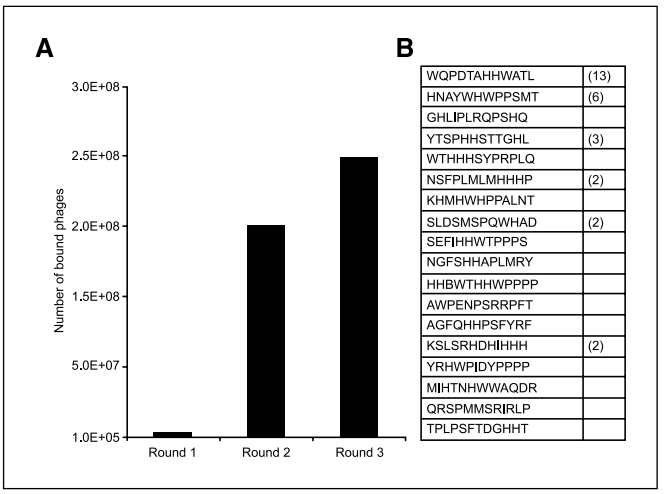

Figure 1. Enrichment of phages binding to PSMA over three rounds of selection. *A,* number of phage bound after each round of selection. *B,* single-letter amino acid sequence of the random insert from each selected phage. *Number in parentheses,* number of phage from sequenced pool (n = 40) containing the unique sequence.

The number of bound phages increased with each round of selection. After the second round of screening, the number of bound phage increased by over three orders of magnitude but increased by less than an order of magnitude after the third round (Fig. 1). Therefore, after this third round, 40 individual phages were sequenced (Fig. 1). More than 30% of the sequenced phages were represented by the peptide sequence WQPDTAHHWATL. A second sequence, HNAYWHWPPSMT, was found in 15% of the sequenced peptides. Ten of 16 sequences contained the motif HHX, whereas one third (6 of 18) of the peptides contained a three amino acid sequence HHW, WHW, HWH, or HWW. Sixteen of 18 sequences had at least one proline residue, whereas 11 of 18 had two or more proline residues (range 2-5). None of the phages had similarity to sequences known to bind to magnetic particles (22). None of the sequences contained multiple acidic amino acids and therefore were unlikely to be PSMA substrates. On the basis of these results, the WQPDTAHHWATL peptide was selected for analysis in further experiments.

Selectivity of binding of WQPDTAHHWATL phage. Two different types of ELISA experiments were done to confirm the selectivity of WQPDTAHHWATL phage binding to PSMA. First, phage binding to immobilized His-PSMA was compared with binding to immobilized BSA (Fig. 2*A*). In this phage ELISA, increasing amounts of WQPDTAHHWATL phage showed much higher binding to immobilized PSMA compared with BSA. The optimal binding differential occurred at a dilution of 10^{10} pfu/mL with almost 10-fold higher binding to PSMA compared with BSA (Fig. 2*A*).

In a second assay, soluble PSMA was used to compete with phage (10^{10}pfu/mL) binding to immobilized proteins (Fig. 2*B*). In this assay, 500 nmol/L soluble His-PSMA inhibited binding of WQPDTAHHWATL phage to immobilized PSMA by >60%. In contrast, soluble BSA had no effect on binding to immobilized PSMA. Additionally, soluble PSMA did not appreciably alter nonspecific binding of phage to immobilized BSA. These results support the conclusion that phage displaying the WQPDTAHHWATL peptide bind selectively to PSMA.

Soluble synthetic WQPDTAHHWATL peptide binds selectively to PSMA. On the basis of the phage-binding results, the WQPDTAHHWATL peptide was synthesized with biotin coupled to the COOH terminus. The COOH terminus was chosen for tagging because the peptide sequences were originally displayed on phage coat surface as NH_2 terminus fusions, suggesting that the NH_2 terminus is involved in binding to PSMA. Incubation of the biotinylated WQPDTAHHWATL peptide with immobilized PSMA or BSA showed significantly higher binding to PSMA at peptide concentrations of 50 and 500 μmol/L (Fig. 3*A*). In contrast, a control consisting of a positively charged 12-amino-acid peptide showed higher overall binding to both proteins but no specific binding to immobilized PSMA compared with BSA (Fig. 3*A, inset*), demonstrating that binding observed with the WQPDTAHHWATL peptide is not based merely on the presence of positively charged residues in the peptide sequence. These results, therefore, suggest that the WQPDTAHHWATL peptide is a low-affinity binding peptide that is relatively selective for PSMA.

Dimerization of WQPDTAHHWATL peptide markedly enhances binding to PSMA and inhibition of enzymatic activity. Screening phage-based peptide libraries to identify sequences that bind to nonpeptide binding proteins (nonreceptors) often yields low-affinity binding ligands (22). In previous studies, our laboratory and others have shown that dimerization of peptides through the use of a lysine residue at the COOH terminus can markedly increase binding affinity due to an avidity effect (20, 23, 24). Therefore, a dimeric form of the WQPDTAHHWATL peptide was synthesized containing biotin at the COOH terminus. The biotinylated monomeric and dimeric peptides were immobilized on streptavidin-coated wells and a reverse ELISA was done by incubation with purified soluble His-PSMA (100 nmol/L). In this

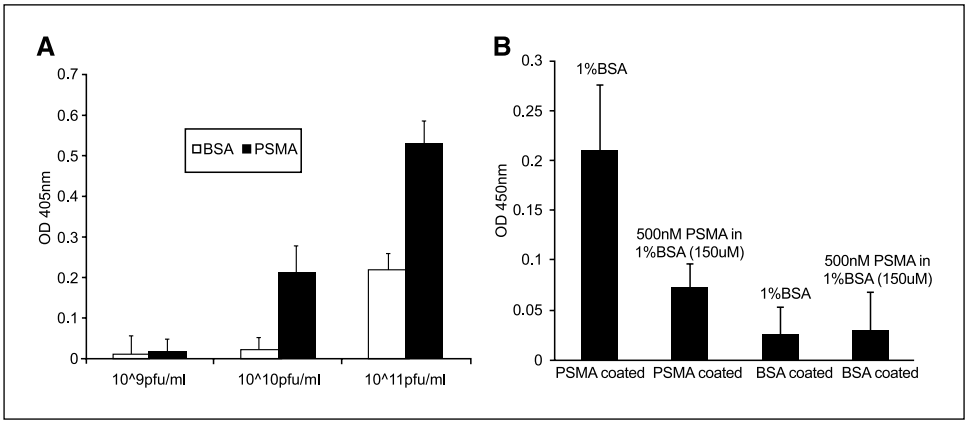

Figure 2. *A,* binding of phage with peptide sequence WQPDTAHHWATL to BSA and PSMA. Recombinant PSMA (0.625 μg) in BSA (25 μg/mL) or BSA alone was immobilized, and indicated dilutions of phages were incubated with immobilized proteins. Extent of binding of anti-M13 antibody to phage bound to PSMA or BSA was determined by addition of HRP substrate OPD and measurement of absorbance at 450 nm. *B,* competitive inhibition with soluble PSMA of WQPDTAHHWATL phage binding to immobilized PSMA. Soluble PSMA (500 nmol/L) was used to compete with PSMA-binding phages containing the WQPDTAHHWATL peptide at concentration of 10^{10} pfu/mL phage. *Columns,* mean binding in four replicate wells each; *bars,* SD.

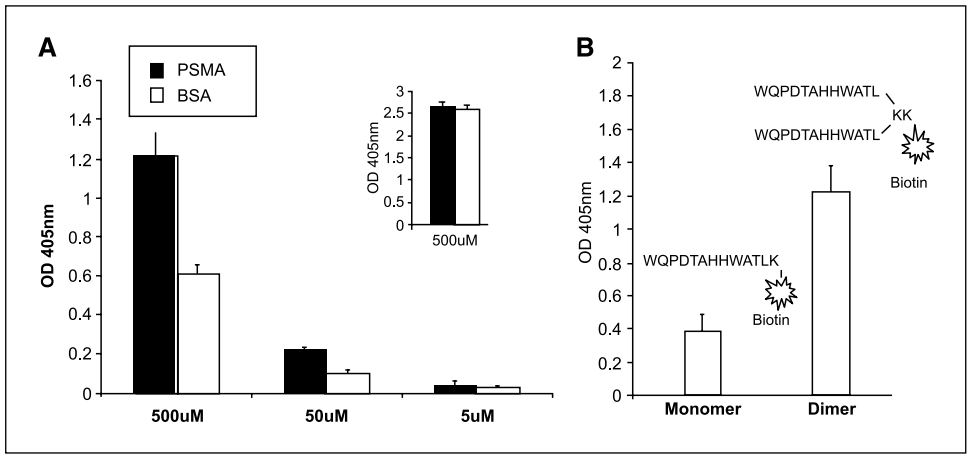

Figure 3. *A,* soluble WQPDTAHHWATLK(biotin) peptide binding to BSA and PSMA. Recombinant PSMA (0.625 μg) and BSA (25 μg/mL) were immobilized and indicated concentrations of the biotinylated WQPDTAHHWATL peptide were incubated with immobilized PSMA or BSA. *Inset,* results from nonselected control peptide QMARIPKRLARHK-biotin assayed for binding using the same procedure. *B,* comparison of PSMA binding to monomeric and dimeric form of the WQPDTAHHWATL peptide. Biotin-labeled monomeric and dimeric peptide were immobilized on streptavidin-coated plates then incubated with His-PSMA (100 nmol/L). *Columns,* mean binding in four replicate wells each; *bars,* SD.

assay, His-PSMA bound significantly better to the dimeric peptide compared with the monomeric (Fig. 3*B*).

WQPDTAHHWATL peptide inhibits enzyme activity of PSMA. Although the aforementioned studies confirmed that the soluble WQPDTAHHWATL peptide could bind PSMA, these studies provide no information as to effect of peptide binding on PSMA function. Functionally, PSMA has been classified as a glutamate carboxypeptidase II (25) with activity as both an *N*-acetylated α-linked acidic dipeptidase (NAALADase; ref. 26) and as a pteroyl poly-γ-glutamyl carboxypeptidase (i.e., folate hydrolase; ref. 27). The NAALADase activity of PSMA can be easily measured by monitoring hydrolysis of the substrate [^{3}H]NAAG, which have very high affinity and specificity for PSMA (K_m = 430 nmol/L and a k_{cat} = 0.6 s^{-1} of protein/min; ref. 21). Therefore, the monomeric and dimeric WQPDTAHHWATL peptides were incubated initially with PSMA for 30 minutes and then [^{3}H]NAAG substrate was added to prevent any NAAG hydrolysis before the peptide is able to bind to PSMA. Control peptides included the QMARIPKRLARH peptide and a short peptide HHWA containing the apparent consensus motif from the phage display. In this study, the monomeric WQPDTAHHWATL peptide was able to inhibit NAAG hydrolysis with an IC_{50} of 23 μmol/L (Fig. 4). In comparison, the dimeric WQPDTAHHWATL peptide inhibited NAAG hydrolysis with an IC_{50} of 2.2 μmol/L (Fig. 4). In contrast, excess control peptides QMARIPKRLARH and HHWA had no effect on NAAG hydrolysis at 100 μmol/L concentration (i.e., <5% inhibition of activity after 30 minutes incubation; data not shown). In a second experiment, cell lysates from PSMA-producing LNCaP were used instead of purified recombinant His-PSMA. PSMA also was inhibited by the monomeric WQPDTAHHWATL peptide at 60 μmol/L in this assay (data not shown), confirming that the WQPDTAHHWATL peptide could also inhibit the full-length membrane-bound form of PSMA.

Binding of WQPDTAHHWATL peptides to PSMA-expressing cell lines. To analyze peptide binding to membrane bound PSMA, fluorescently labeled peptides were synthesized by coupling FITC to the COOH terminus of either the monomeric or dimeric peptide. Previously, we had characterized PSMA expression and enzymatic activity of human prostate cancer cell lines and, based on this analysis, selected two lines, LNCaP and CWR22R, that produced measurable levels of enzymatically active PSMA and two lines, PC-3 and DU145, that did not. WQPDTAHHWATL monomeric and dimeric peptides were incubated with these prostate cancer cell lines at varying concentrations (i.e., 1, 5, 10, and 50 μmol/L) in tissue culture medium containing 1% FBS as a blocking agent. In this assay, binding of the monomeric WQPDTAHHWATL peptide above background autofluorescence could not be observed at any of the tested concentrations (Fig. 5). In contrast, cell binding of the dimeric WQPDTAHHWATL peptide could be easily visualized at concentrations as low as 5 μmol/L (Fig. 5). Labeled, dimeric peptide bound to a similar degree to both CWR22R and LNCAP. In contrast, no significant binding of fluorescent-labeled WQPDTAHHWATL dimeric peptide above background to non-PSMA–expressing prostate cancer cells was observed (Fig. 5).

Modeling the structure of the dimeric peptide. Previously, it has been proposed that PSMA is active only in its dimeric form (7), which possesses two catalytic sites that could potentially be targeted better by a dimeric peptide that bridged the two binding sites. Experimentally, we observed that the dimeric version of the peptide is a ~10-fold better inhibitor of PSMA than the monomer. Therefore, we did a careful analysis of the crystal structure of the PSMA dimer (Protein Data Bank code 1Z8L) to evaluate whether each arm of the dimeric peptide could bind separately to each

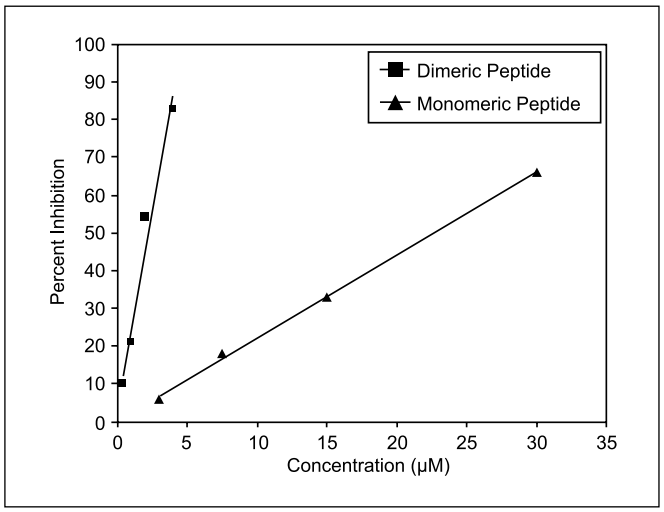

Figure 4. Inhibition of NAALADase activity of PSMA by monomeric and dimeric peptides. His-PSMA hydrolysis of [^{3}H]NAAG was assayed as described in Materials and Methods in the absence or presence of indicated concentration of monomeric or dimeric peptide. After 15 minutes of incubation at 37°C, the amount of released [^{3}H]Glu was determined. Percentage inhibition is the ratio of amount of [^{3}H]Glu released in presence of peptide compared with control (i.e., His-PSMA only). *Points,* average of duplicate experiments. Best-fit line is included.

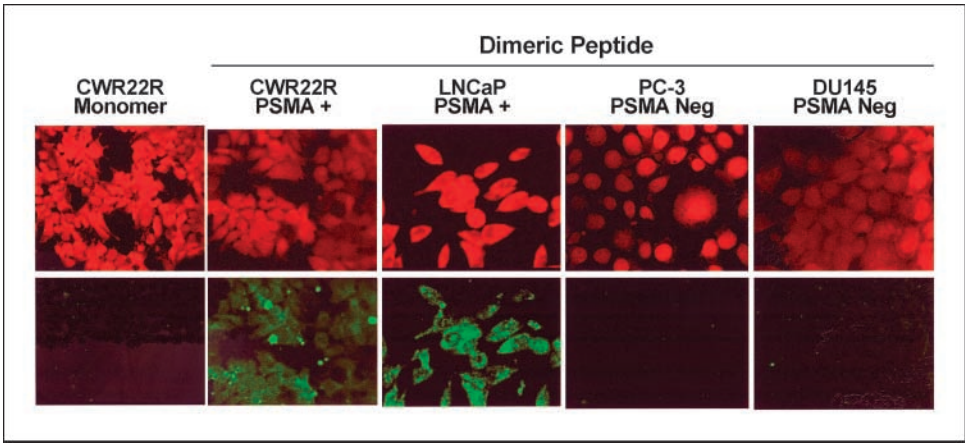

Figure 5. Dimeric WQPDTAHHWATL peptide binds selectively to PSMA-producing prostate cancer cells. Attached PSMA-positive (LNCaP, CWR22R) and PSMA-negative (PC-3, DU145) human prostate cancer were prelabeled with Orange Cell Tracker (Invitrogen) at 2.5 μmol/L in RPMI for 30 minutes. After washing with HBSS, cells were incubated with FITC-labeled monomeric (50 μmol/L) or dimeric (5 μmol/L) WQPDTAHHWATL peptide in 1% FCS containing medium for 1 hour. Cells were washed thrice with PBS and fixed with 1% formalin for 0.5 hour at room temperature. Cells were visualized using Zeiss Meta 510 confocal microscope at ×20 magnification. *Top,* orange cell tracker–labeled cells (rhodamine filter set); *middle,* labeled peptide binding (FITC filter set); *bottom,* overlay of both panels.

protein monomer in the crystal structure. This type of binding of a dimeric peptide to a protein dimer has been observed before in the case of an erythropoietin mimetic peptide binding to the dimer interface of the erythropoietin receptor (22). The crystal structure analysis of PSMA, however, revealed that the catalytic binding sites of each protein monomer face opposite to each other with the distance between two similar Zn^{2+} atoms in the catalytic site of each monomer being 56 Ångstrom. Thus, the orientation of the catalytic sites and the large distance between them rule out the possibility of this 12-amino-acid dimeric peptide binding the catalytic site of both protein monomers simultaneously. This observation, instead, favors a binding mode in which one dimeric peptide binds in the vicinity of only one catalytic site in the PSMA dimer.

To understand the role of peptide secondary structure on the PSMA inhibition, we have modeled the solution structure of dimeric peptide (Fig. 6*A*). In this model, two arms of peptide are brought close to each other via coordination of a divalent cobalt cation by two histidines located on each arm. Due to steric considerations, the other two histidine residues cannot participate in the metal coordination at the same time and remain solvent exposed whereby they are free to coordinate with other metal ions. This possibly explains why the higher concentration of cobalt results in the aggregation and precipitation of the peptide substrates. The energy minimized structure adopts a β-turn like loop on the NH_2-terminal side of each arm, which brings the tryptophan and asparatic side chains on the same side. The β-turn like structure at the NH_2 terminus of peptide agrees with observation that the NH_2-terminal sequence QPD is similar to nonnative β-turn sequence, which has been implicated in nucleating the formation of a β-hairpin in peptides derived from the NH_2 terminus of ubiquitin (28).

The β-turn–like structure of the peptide at the NH_2 terminus is consistent with the shape of the catalytic binding cavity, which is narrow and covers much less surface area than the entire PSMA dimer surface (Fig. 6*B*). To discover the binding mode of NH_2-terminal residues in the dimeric peptide, we docked the WQPDTA motif in the catalytic site of PSMA using the program GOLD v3.0. To preclude any personal bias, the binding mode with the highest GOLD score (47.8) was chosen to be the best representative of the true binding mode.

The catalytic site of PSMA is polar mostly due to an arginine patch where a series of arginine residues are clustered within 4.5 Å of each other and 6 to 12 Å away from the nearest zinc atom. Figure 6*C* presents the binding mode of the WQPDTA motif in the catalytic site. W1 of the peptide is docked opposite to the arginine patch in a shallow hydrophobic pocket located at the interface of apical and helical domain formed mainly by Phe^{209}, Tyr^{700}, and the aliphatic side chain of Lys^{207}. This explains why a hydrophobic residue such as W1 can be accommodated in a mostly polar binding site. The free amine at the NH_2 terminus is in a position to make a hydrogen bond with Tyr^{234} and Gln^{254}. The carboxy side chain of D4 is oriented toward the catalytic water and is the closest

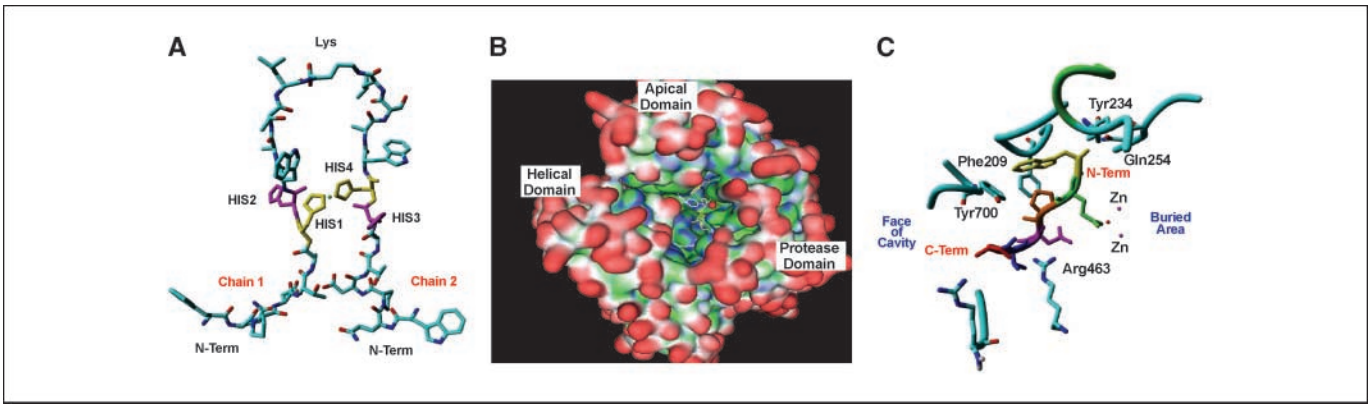

Figure 6. *A,* the solution structure of dimeric peptide $(WQPDTAHHWATL)_2$-K. *Yellow,* metal-coordinating histidine residues; *magenta,* histidines exposed to the solvent; *green,* cobalt ion. *B,* the molecular surface representation of the PSMA catalytic site. *Yellow,* the docked peptide moiety; *white,* the protein residues interacting with the peptide. *C,* the binding mode of WQPDTA peptide moiety. W1 (*yellow*), Q2 (*green*), P3 (*orange*), D4 (*purple*), T5 (*blue*), and A6 (*red*). The orientation of PSMA monomer is such that face of binding cavity is facing left, whereas the buried area at the bottom of catalytic side containing zinc ions is on the right side.

to the zinc atoms. The side chain of D4 is docked in the arginine patch, making a hydrogen bond with Arg^{463}, which might be critical for the overall binding of the peptide. The COOH-terminal part of the WQPDTA motif, including T5 and A6, docks in a groove formed at the interface of helical and protease domain. The side chain hydroxyl of T5 residue is in perfect position to make a hydrogen bond with Asp^{465}.

The COOH terminus of the WQPDTA motif lies above Arg^{511} and is oriented toward the groove located between helical and protease domain. This suggests that the HHWATL motif at the COOH terminus of docked motif will be positioned outside the catalytic site toward this groove. The positioning of the COOH terminus of the docked motif validates the authenticity of the unbiased binding mode as, although the docking calculations were blind to the presence of HHWATL motif at the COOH terminus, the binding mode still allowed for the presence for extra residues at the COOH terminus.

Discussion

Phage display of random peptide libraries has been used successfully in a number of applications that include identification of protein-binding ligands, optimization of antibody binding, and identification of substrates for proteases (29–32). The goal of this study was to use a phage library containing a random linear peptide displayed at the amino terminus of the coat protein III to identify peptides that bind specifically to the prostate tissue differentiation protein and cancer marker PSMA. The ultimate goal of this process is to use these peptides identified by this phage display methodology that can be used to deliver drugs or cytotoxic molecules to cancer cells (33).

Because the intended target for this targeting strategy is the extracellular portion of the PSMA protein, in this study we generated a soluble, His-tagged PSMA protein that lacked the transmembrane and intracellular domains of PSMA. We used a solution phase screening of phage display library of 12-amino-acid-long peptides to select for peptides binding to recombinant His-tagged PSMA. Such solution screening promotes affinity discrimination and yields peptides with higher binding affinities compared with solid-phase panning methodologies (22). In this study, the use of the solution-phase screening method may explain why maximum enrichment of the library for PSMA binding was obtained after the first round of screening.

The peptide sequences obtained from this screening were compared with the known target-unrelated peptides frequently recovered in the screening of phage-displayed random peptide libraries with antibodies (34). Also, there was no sequence similarity to known peptides that bind to magnetic particles (22). Forty selected phages were sequenced and one sequence, WQPDTAHHWATL, was identified that contributed to >30% of the sequenced phages. In addition, 23 of 40 of the peptide sequences contained one of three tripeptide motifs HHW, WHW, and HWH. The peptide motif HHX was observed in ~60% of the unique sequences or 25 of 40 total sequences. This dihistidine peptide motif had also emerged as part of a consensus PSMA-binding sequence (i.e., CQKHHNYLC) identified previously in a phage display–based screening of a cyclic six-amino-acid peptide library (35).

In this study, the WQPDAHHWATL peptide showed selectivity of binding to PSMA based on ELISA-based plate assays and the binding of this peptide to surface-bound PSMA could be competed off by soluble PSMA. Although discrete binding affinity was not calculated for this peptide, the IC_{50} for inhibition of PSMA NAALADASE activity was 23 μmol/L. This type of low-affinity nonoptimized binding is of the same order of magnitude observed in other studies using phage display to select peptide binding to nonreceptor proteins. Previously, it had been shown by many groups, including our own, that the peptide-binding affinity can be improved by increasing the binding avidity through use of multivalent binding strategies, such as dimeric or tetrameric peptides or streptavidin-biotinylated peptide tetramers (20, 23, 24). Dimerization of the WQPDAHHWATL peptide resulted in significant enhancement of PSMA binding compared with the monomeric form.

The dimeric peptide also showed inhibition of PSMA enzymatic activity at 10-fold lower concentrations. In addition, binding of a fluorescently labeled dimeric peptide selectively to PSMA-producing prostate cancer cells compared with non-PSMA-producing cells could be easily visualized at a peptide concentration of 5 μmol/L, whereas no binding of the fluorescently tagged monomeric peptide was observed at concentrations up to 50 μmol/L. These results support prior observations that binding characteristics of peptides identified by phage display techniques can be greatly enhanced through generation of dimeric or multivalent peptides. In this regard, a dimeric or multivalent form of the PSMA-binding peptide will be used in future applications that will include drug or viral targeting, imaging, etc.

The sequence analysis of all the peptides selected by the phage display reveals that there is an overabundance of histidines and prolines. The presence of histidines in most of the peptides is intriguing as histidine residues are known to chelate divalent metal ions, including zinc. The PSMA catalytic binding site contains two zinc ions that can potentially be chelated by these histidines, leading to inactivation of the enzyme. However, the experimental data seems to exclude this mechanism for binding as the short peptide HHWA did not possess any inhibitory potency toward PSMA.

Histidines have also been found abundant in earlier phage display binding studies directed toward other nonmetalloprotease systems (36–38). These observations led us to hypothesize that the histidines in the WQPDTAHHWATL peptide are not directly involved in PSMA binding. Rather, they help the dimeric peptide chains adopt a particular configuration that is favorable for PSMA binding. This can be achieved via histidines interacting with the divalent cations abundant in the assay buffers, such as cobalt, and modulating the structure of the peptide especially when in the dimeric form. This hypothesis is strongly favored by an earlier nuclear magnetic resonance study on the PSMA substrate and neurodipeptide NAAG that concluded that metal binding has important consequences for the solution structure of these dipeptides and their ability to act as PSMA substrates (39). For the WQPDTAHHWATL peptide, the dimeric form brings four histidines into close vicinity. This can lead to efficient coordination of a divalent cation, such as cobalt, by the dimer and result in the adoption of a favorable configuration for binding and subsequent inhibition of PSMA.

The high frequency of prolines in the phage peptides further supports this model as prolines are important for peptide folding via production of turns in the protein chain. Prolines also reduce the conformation flexibility of a peptide as they can only assume limited number of allowed torsion angles in a Ramachandran plot. Reducing the conformational flexibility of peptide chain has important

consequences for binding as it reduces the entropic penalty for binding to a protein target. The importance of peptide flexibility and entropic penalty in PSMA inhibition has been recognized before in a study that concluded that difference in inhibitory potency of PSMA inhibitors was largely entropy based (40).

Modeling of WQPDTAHHWATL sequence showed that the proline in the peptide produces a β-turn–like structure at the NH_2 terminus that is consistent with the shape of the narrow catalytic binding cavity of PSMA. The binding of peptides to such a cavity will result in severe torsion in the peptide chain and loss of conformational flexibility resulting in a high entropic penalty for flexible peptides. Therefore, the dimeric peptide with the combination of divalent cation complex formation with dihistidines and the proline-induced β-turns results in stabilization of the peptide into a less flexible, more entropically favorable conformation that enhances binding characteristics compared with the monomeric peptide.

In conclusion, these results show that the dimerization of the PSMA-binding peptide enhances PSMA inhibition ~10-fold compared with the monomeric peptide. Modeling studies suggest that this enhanced binding is due to stabilization of the peptide into a less flexible conformation. This stabilization is similar to what occurs with cyclization of peptides using flanking cysteine residues. Further studies are under way to confirm the modeling results by studying binding of peptide lacking the HHW motif. If these studies support the model, they would suggest a strategy to optimize binding in which the HHWATL portion of the peptide is fixed in the phage sequence, whereas the remaining amino acids are randomized. Peptides selected by this second round of phage screening can also be tested as dimers in solution and binding compared with that of the WQPDTA peptide. In addition, dimeric peptide could be synthesized in which each "arm" of the peptide contains a unique binding sequence.

Acknowledgments

Received 4/26/2006; revised 6/23/2006; accepted 7/14/2006.

Grant support: David H. Koch Award from the Prostate Cancer Foundation (S.R. Denmeade).

The costs of publication of this article were defrayed in part by the payment of page charges. This article must therefore be hereby marked *advertisement* in accordance with 18 U.S.C. Section 1734 solely to indicate this fact.

We thank Carrie Jenkins for excellent assistance in the preparation of the manuscript, and Rebecca Ricklis and Marc Rosen for excellent technical assistance.

References

1. Fair WR, Israeli RS, Heston WD. Prostate-specific membrane antigen. Prostate 1997;32:140–8.
2. Kawakami M, Nakayama J. Enhanced expression of prostate-specific membrane antigen gene in prostate cancer as revealed by *in situ* hybridization. Cancer Res 1997;57:2321–4.
3. Silver DA, Pellicer I, Fair WR, et al. Prostate-specific membrane antigen expression in normal and malignant human tissues. Clin Cancer Res 1997;3:81–5.
4. Bander NH, Milowsky MI, Nanus DM, et al. Phase I trial of 177lutetium-labeled J591, a monoclonal antibody to prostate-specific membrane antigen, in patients with androgen-independent prostate cancer. J Clin Oncol 2005;23:4591–601.
5. Mhaka A, Gady AM, Rosen DM, et al. Use of methotrexate-based peptide substrates to characterize the substrate specificity of prostate-specific membrane antigen (PSMA). Cancer Biol Ther 2004;3:551–8.
6. Davis MI, Bennett MJ, Thomas LM, et al. Crystal structure of prostate-specific membrane antigen, a tumor marker and peptidase. Proc Natl Acad Sci U S A 2005;102:5981–6.
7. Schulke N, Varlamova OA, Donovan GP, et al. The homodimer of prostate-specific membrane antigen is a functional target for cancer therapy. Proc Natl Acad Sci U S A 2003;100:12590–5.
8. O'Keefe DS, Bacich DJ, Heston WD. Comparative analysis of prostate-specific membrane antigen (PSMA) versus a prostate-specific membrane antigen-like gene. Prostate 2004;58:200–10.
9. Cunha AC, Weigle B, Kiessling A, et al. Tissue-specificity of prostate specific antigens: comparative analysis of transcript levels in prostate and non-prostatic tissues. Cancer Lett 2006;236:229–38.
10. Dumas F, Gala JL, Berteau P, et al. Molecular expression of PSMA mRNA and protein in primary renal tumors. Int J Cancer 1999;80:799–803.
11. Gala JL, Loric S, Guiot Y, et al. Expression of prostate-specific membrane antigen in transitional cell carcinoma of the bladder: prognostic value? Clin Cancer Res 2000;6:4049–54.
12. Liu H, Moy P, Kim S, et al. Monoclonal antibodies to the extracellular domain of prostate-specific membrane antigen also react with tumor vascular endothelium. Cancer Res 1997;57:3629–34.
13. Chang SS, Reuter VE, Heston WD, et al. Five different anti-prostate-specific membrane antigen (PSMA) antibodies confirm PSMA expression in tumor-associated neovasculature. Cancer Res 1999;59:3192–8.
14. Huang X, Bennett M, Thorpe PE. Anti-tumor effects and lack of side effects in mice of an immunotoxin directed against human and mouse prostate-specific membrane antigen. Prostate 2004;61:1–11.
15. Nanus DM, Milowsky MI, Kostakoglu L, et al. Clinical use of monoclonal antibody HuJ591 therapy: targeting prostate specific membrane antigen. J Urol 2003;170:S84–8; discussion S88–9.
16. Leuschner C, Enright FM, Gawronska-Kozak B, et al. Human prostate cancer cells and xenografts are targeted and destroyed through luteinizing hormone releasing hormone receptors. Prostate 2003;56:239–49.
17. Schally AV, Nagy A. New approaches to treatment of various cancers based on cytotoxic analogs of LHRH, somatostatin and bombesin. Life Sci 2003;72:2305–20.
18. Grifman M, Trepel M, Speece P, et al. Incorporation of tumor-targeting peptides into recombinant adeno-associated virus capsids. Mol Ther 2001;3:964–75.
19. Barbas CF, Burton DR, Scott JK, Silverman GJ. Phage display: a laboratory manual. Cold Spring Harbor (New York): Cold Spring Harbor Laboratory Press; 2000.
20. Aggarwal S, Janssen S, Wadkins RM, et al. A combinatorial approach to the selective capture of circulating malignant epithelial cells by peptide ligands. Biomaterials 2005;26:6077–86.
21. Tiffany CW, Lapidus RG, Merion A, et al. Characterization of the enzymatic activity of PSM: comparison with brain NAALADase. Prostate 1999;39:28–35.
22. Gebhardt K, Lauvrak V, Babaie E, et al. Adhesive peptides selected by phage display: characterization, applications and similarities with fibrinogen. J Pept Res 1996;9:269–78.
23. Cwirla SE, Balasubramanian P, Duffin DJ, et al. Peptide agonist of the thrombopoietin receptor as potent as the natural cytokine. Science 1997;276:1696–9.
24. Wrighton NC, Balasubramanian P, Barbone FP, et al. Increased potency of an erythropoietin peptide mimetic through covalent dimerization. Nat Biotechnol 1997;15:1261–5.
25. Luthi-Carter R, Barczak AK, Speno H, et al. Molecular characterization of human brain N-acetylated α-linked acidic dipeptidase (NAALADase). J Pharmacol Exp Ther 1998;286:1020–5.
26. Carter RE, Feldman AR, Coyle JT. Prostate-specific membrane antigen is a hydrolase with substrate and pharmacologic characteristics of a neuropeptidase. Proc Natl Acad Sci U S A 1996;93:749–53.
27. Pinto JT, Suffoletto BP, Berzin TM, et al. Prostate-specific membrane antigen: a novel folate hydrolase in human prostatic carcinoma cells. Clin Cancer Res 1996;2:1445–51.
28. Jourdan M, Griffiths-Jones SR, Searle MS. Folding of a β-hairpin peptide derived from the NH_2 terminus of ubiquitin. Conformational preferences of β-turn residues dictate non-native β-strand interactions. Eur J Biochem 2000;267:3539–48.
29. Arap W, Kolonin MG, Trepel M, et al. Steps toward mapping the human vasculature by phage display. Nat Med 2002;8:121–7.
30. El-Mousawi M, Tchistiakova L, Yurchenko L, et al. A vascular endothelial growth factor high affinity receptor 1-specific peptide with antiangiogenic activity identified using a phage display peptide library. J Biol Chem 2003;278:46681–91.
31. Pan W, Arnone M, Kendall M, et al. Identification of peptide substrates for human MMP-11 (stromelysin-3) using phage display. J Biol Chem 2003;278:27820–7.
32. Smith GP, Petrenko VA. Phage display. Chem Rev 1997;97:391–410.
33. Aina OH, Sroka TC, Chen ML, et al. Therapeutic cancer targeting peptides. Biopolymers 2002;66:184–99.
34. Menendez A, Scott JK. The nature of target-unrelated peptides recovered in the screening of phage-displayed random peptide libraries with antibodies. Anal Biochem 2005;336:145–57.
35. Lupold SE, Rodriguez R. Disulfide-constrained peptides that bind to the extracellular portion of the prostate-specific membrane antigen. Mol Cancer Ther 2004;3:597–603.
36. Dreier B, Segal DJ, Barbas CF III. Insights into the molecular recognition of the 5′-GNN-3′ family of DNA sequences by zinc finger domains. J Mol Biol 2000;303:489–502.
37. Eteshola E, Brillson LJ, Lee SC. Selection and characteristics of peptides that bind thermally grown silicon dioxide films. Biomol Eng 2005;22:201–4.
38. Rodi DJ, Soares AS, Makowski L. Quantitative assessment of peptide sequence diversity in M13 combinatorial peptide phage display libraries. J Mol Biol 2002;322:1039–52.
39. Lannom HK, Dill K, Denarie M, et al. 13C n.m.r. study of the structure and the metal ion binding sites of neuropeptides composed of L-Asp and L-Glu. Int J Pept Protein Res 1986;28:67–78.
40. Oliver AJ, Wiest O, Helquist P, et al. Conformational and SAR analysis of NAALADase and PSMA inhibitors. Bioorg Med Chem 2003;11:4455–61.

A Dimeric Peptide That Binds Selectively to Prostate-Specific Membrane Antigen and Inhibits its Enzymatic Activity

Saurabh Aggarwal, Pratap Singh, Ozlem Topaloglu, et al.

Cancer Res 2006;66:9171-9177.